Dynamics in electron-impact ionization of H_2O

D. S. Milne-Brownlie,[1] S. J. Cavanagh,[2] Birgit Lohmann,[1] C. Champion,[3] P. A. Hervieux,[3] and J. Hanssen[3]
[1]*School of Science, Griffith University, Nathan, Queensland, Australia 4111*
[2]*Research School of Physical Sciences and Engineering, Australian National University, Canberra, Australian Capital Territory 0200, Australia*
[3]*Laboratoire de Physique Moléculaire et des Collisions, Institut de Physique, 1 Boulevard Arago, Technopôle 2000, 57078 Metz Cedex 3, France*
(Received 5 December 2003; published 5 March 2004)

We present multiply differential cross sections for electron-impact ionization of the water molecule. The experimental results are compared with theoretical cross sections calculated using a recently developed distorted-wave Born approach for molecules. The experimental cross sections exhibit a very large recoil scattering, which is not predicted by the theory. This has implications for applications of this theoretical approach in areas such as modeling of ionization in biological systems.

DOI: 10.1103/PhysRevA.69.032701 PACS number(s): 34.80.Dp

Electron-impact ionization is an important fundamental collision process which plays a significant role in areas as diverse as plasma physics, astrophysics, atmospheric modeling, discharge physics, and radiobiology. Electron-electron coincidence [or $(e,2e)$] experiments provide complete kinematic information about the collision process, and electron-impact ionization of atoms has been studied extensively using this technique. The direct, single-ionization process may be represented as

$$e_0 + A \rightarrow A^+ + e_A + e_B,$$

where the subscripts refer to the incident, scattered, and ejected electrons, respectively, and A represents the target under investigation. The quantity measured in the coincidence experiments is proportional to the triple-differential cross section (TDCS), which describes the angular distribution of ejected electrons of specific energy, for selected incident and scattered electron momenta. For molecular targets, a large body of data exists from electron momentum spectroscopy (EMS) studies. EMS uses the electron-electron coincidence technique to probe the electronic structure of the target (see, for example, Ref. [1] and references therein). EMS studies require the selection of kinematic conditions which allow a straightforward transformation between the measured cross section and the momentum probability distribution in the target. On the other hand, dynamical studies of the $(e,2e)$ process in molecules have been sparse, mainly due to the difficulty in modeling this process theoretically. Very sophisticated theoretical calculations are available to describe the ionization process for atoms, but incorporating molecular target wave functions into such calculations has to date proven to be an almost intractable problem. Dynamical studies of molecular ionization have been performed on H_2 [2,3], N_2 [2,4–6], CO [6], N_2O [7], and O_2 [8]. The theoretical approaches used to describe the experimental data included the plane-wave impulse approximation, first Born approximation, and first Born with orthogonalized Coulomb waves. At high incident energies, the first Born and impulse approximations were found to perform reasonably well, however these methods are not very reliable at lower energies. In recent breakthroughs, distorted-wave approximation calculations have appeared for electron-impact ionization of H_2 [9] and H_2O [10], targeting the low- to intermediate-energy region.

The water molecule is a very interesting target. As water constitutes $\approx$80% of biological material, there is considerable interest in cross sections for electron-impact ionization of water for use in charged particle track structure analysis; the latter is used in modeling radiation damage in biological samples. To this end, Champion *et al.* [10] calculated multiply differential cross sections for electron-impact ionization of the water molecule, using a distorted-wave Born approximation. In these calculations, the initial state is described by the product of a plane-wave and molecular target wave functions; the latter formulated using a linear combination of atomic orbitals. The molecular wave function is centered on the oxygen atom. The (slow) ejected electron is described by a distorted wave, while the (fast) scattered electron is represented by a plane wave. In the case of total cross sections, single-differential cross sections (SDCS), and double-differential cross sections they found reasonable agreement with the available experimental data. However, although the water molecule has been investigated using EMS [11,12], no dynamical studies of the TDCS for electron-impact ionization of H_2O existed for comparison with their calculations. As they point out, these cross sections are very important in tracking the history of an incident particle and the products of the collision in terms of energy deposits and angular distributions. The importance of such information is illustrated in Ref. [13], in which it was shown that low-energy secondary electrons in the energy range 3–20 eV, produced in a primary ionization event, can induce substantial single- and double-DNA strand breaks. As water is the ambient medium in most biological systems, knowledge of the production mechanisms for low-energy secondary electrons from a primary ionization event in a water molecule is of particular importance.

In this paper we present measurements of the TDCS for electron-impact ionization of vapor phase water molecules. The experimental data are compared with distorted-wave cal-

culations of the TDCS, calculated using the approach described in Ref. [10]. The results provide insights into the behavior of these cross sections for this important molecular target, and into the utility of this theoretical approach in predicting TDCS for molecular ionization.

The experiments were performed in an electron coincidence spectrometer [14] in which an incident electron beam crosses a target gas jet at right angles. The outgoing electrons from the ionization event enter two hemispherical electron-energy analyzers. The two analyzers are mounted on independently rotatable turntables which are concentric with the interaction region. The electrons exiting the analyzers are detected by charged particle detectors, with the higher-energy (scattered) electron being detected by a channel electron multiplier, and the low-energy ejected electron being detected by a position-sensitive detector [15]. Coincidence fast timing electronics [15] are used to determine if two detected electrons are correlated (arise from the same scattering event). The experiments reported here were performed in the coplanar asymmetric geometry, in which the incident and outgoing electrons all lie in the same plane, and the scattered electron is detected at a fixed forward angle, while the ejected electron-energy analyzer is rotated in the plane.

The water vapor target enters the interaction region through a 0.69 mm diameter stainless steel capillary. The water reservoir is a glass vial which contains high-performance liquid-chromatography grade water. A process of LN_2 freezing and subsequent thawing of the water was undertaken to remove gas contaminants. The experiment was conducted at elevated temperatures of 40 °C and 50 °C for the scattering chamber and water gas lines, respectively.

The experiments were performed at an incident energy of 250 eV, ejected electron energy of 10 eV, and scattered electron detection angle of 15°. The energy at which the scattered electron must be detected is determined by energy conservation, such that

$$E_0 = E_a + E_b + \varepsilon_i,$$

where E_0 is the incident energy, E_a is the scattered electron energy, E_b is the ejected electron energy, and ε_i is the binding energy of the orbital being ionized. The electronic structure of the water molecule consists of five orbitals: two atomiclike orbitals ($1a_1$ and $2a_1$) and three molecular orbitals ($1b_2$, $3a_1$, and $1b_1$). We have measured the TDCS for electron-impact ionization of the $1b_1$, $3a_1$, $1b_2$, and $2a_1$ orbitals, with binding energies of 12.6 eV, 14.7 eV, 18.5 eV, and 32.2 eV, respectively. As a position-sensitive detector is used to detect the slow ejected electron, it is possible to measure simultaneously a range of energies for this outgoing electron. Figure 1 shows a coincidence binding energy spectrum, corresponding to detection of the scattered electron at a fixed energy, and a range of energies for the ejected electron. The binding energy spectrum shows two peaks, one due to coincidence detection of an electron ejected from the $1b_1$ orbital with a kinetic energy of 10 eV, while the second peak corresponds to detection of an electron ejected from the $3a_1$ orbital with a lower energy of $\approx$8 eV. As can be seen from Fig. 1, the coincidence energy resolution of the apparatus is such that these

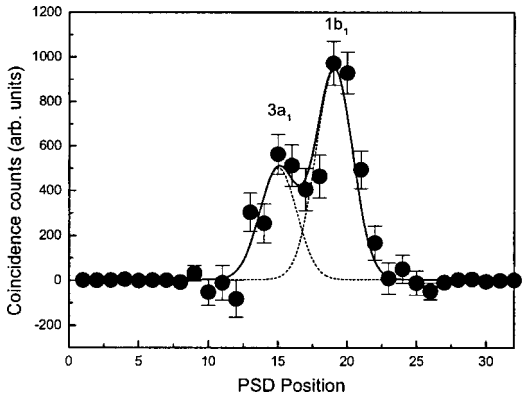

FIG. 1. Coincidence binding-energy spectrum of the outermost two molecular orbitals of water, fitted with a sum of two Gaussians. The data are plotted as a function of position (channel number) across the position-sensitive detector.

two peaks are not entirely resolved, however it is possible to fit the spectrum with two Gaussians, as shown. Using the fitted spectrum, we can extract information about the two orbitals separately.

Figures 2(a)–2(e) show our experimental results for the triple-differential cross section for electron-impact ionization of the water molecule. The results are compared with new calculations corresponding to the kinematic conditions used in the experiments. Note that the angular distribution can be divided into two main regions: the binary region, from 0° to 180°, and the recoil region, from 180° to 360°. The binary region is so called because the structures in this angular range arise from single binary collisions. In contrast, the structures in the recoil region are believed to be due to a process in which the ejected electron produced in an initial binary collision subsequently undergoes a recoil scattering from the nucleus, resulting in the two correlated electrons emerging on the same side of the incident electron beam.

The angular distributions in these two regions are obtained by moving the scattered electron-energy analyzer from −15° to +15°, and the normalization between the two regions is determined in a separate experiment (see Ref. [16] for details). One of the experimental problems which arises in using a water vapor target is instability in the target pressure in the interaction region. The result is that determination of the binary-to-recoil ratio is more difficult than in the case of a "well-behaved" rare gas target. We estimate that the error in the binary/recoil ratio ranges from 30% to 40%. The theoretical calculations are presented in each case by the solid lines. The TDCS has been calculated for each orbital separately. As our experimental results are on a relative scale, in each figure they have been normalized to the theoretical calculation in the binary region so as to give the best visual fit.

Figure 2(a) shows the summed cross section for electron-impact ionization of both the $1b_1$ and $3a_1$ orbitals. Figures 2(b) and 2(c) are the TDCS in the binary region for the separate $1b_1$ and $3a_1$ orbitals; the experimental data were extracted by fitting two Gaussians to the binding energy spectra at each angle. Due to the greater scatter in the binding energy data in the recoil region, it was not possible to

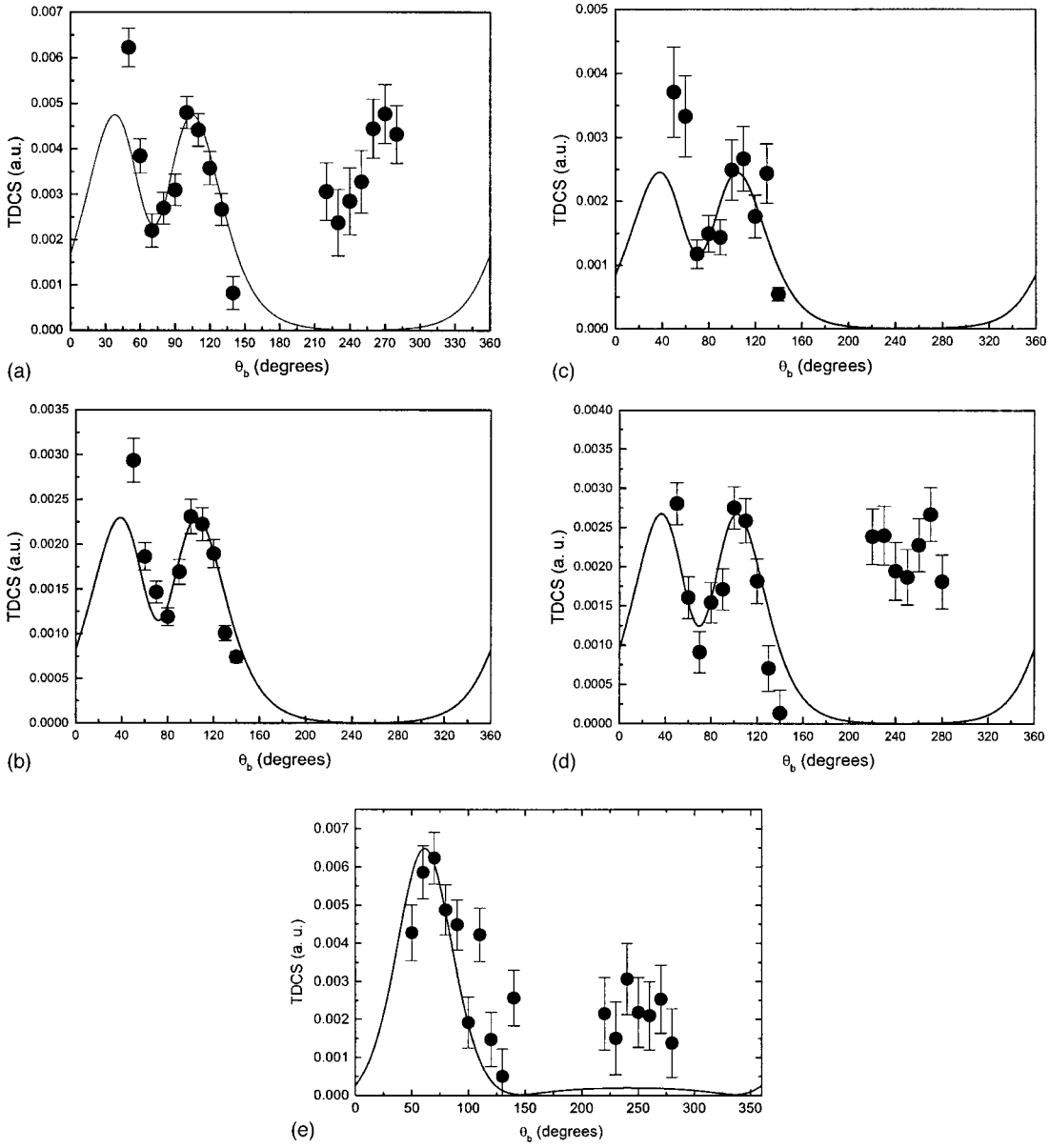

FIG. 2. (a) Summed TDCS for electron-impact ionization of the $1b_1$ and $3a_1$ orbitals of H_2O. The points are the experimental data, while the solid curve is the theory. The incident electron energy is 250 eV, ejected electron energy is 10 eV, and the scattering angle is 15°. (b) TDCS for electron-impact ionization of the $1b_1$ orbital. Points are the experimental data while the solid line is the theory. Kinematic conditions as for (a). (c) TDCS for electron-impact ionization of the $3a_1$ orbital. Points are the experimental data while the solid line is the theory. Kinematic conditions as for (a), except that in the experiment, the ejected electron has an energy of 8 eV. (d) TDCS for electron-impact ionization of the $1b_2$ orbital. Points are the experimental data while the solid line is the theory. Kinematic conditions as for (a). (e) TDCS for electron-impact ionization of the $2a_1$ orbital. Points are the experimental data while the solid line is the theory. Kinematic conditions as for (a).

unambiguously separate the two orbitals in this angular range, and hence only the binary region is presented.

It is immediately apparent that the theory is very successful in describing the shape of the TDCS in this angular range, albeit with some discrepancy in the relative magnitudes of the two binary peaks. However, it is also apparent that there is no agreement in the recoil region, and indeed the theory predicts essentially no recoil structure, whereas in fact the recoil scattering is almost equal in magnitude to the binary scattering for these kinematics.

The main features in the cross section are the double peak in the binary region and the single, almost equally large, recoil peak. The double-peak structure in the binary region is consistent with the designation of the outer valence orbitals as primarily $2p$ in character [10]. The double-peak structure is observed for ionization of p orbitals in atomic targets, and is a reflection of the form of the momentum probability density distribution of the electrons in these orbitals (the character of the various orbitals in water has been identified previously [11]). It is interesting to note the remarkably similar shape of the cross section in the binary region (experimental and theoretical) for the two outermost orbitals.

Figure 2(d) shows the TDCS for electron-impact ionization of the innermost molecular orbital, the $1b_2$ orbital. The form of the TDCS is very similar to that for the outer valence orbitals, with a double binary peak and large recoil peak. Again, the $1b_2$ is predicted to be of predominantly $2p$ character, which is borne out by the presence of the split binary peak. The theoretical calculation very successfully describes the binary region, but completely misses the recoil intensity. The final orbital we have investigated is the $2a_1$ atomiclike orbital [Fig. 2(e)]. This orbital arises primarily from the oxygen $2s$ electrons. Although the data are rather scattered, it is clear that the TDCS in this case exhibits a single binary and single recoil peak. (Note that the difficulty of the measurements increases as the binding energy increases, since the SDCS goes down.) Again, the calculation predicts the binary structure quite well, but although there is a hint of a recoil peak in the theoretical results, the intensity is again significantly underestimated. The experimental results clearly indicate that considerable intensity is directed into the recoil region, and this is not accounted for by the calculations.

The inability of the theory to account for the recoil scattering is most likely related to the use of plane waves in the incident and fast outgoing channels. Calculations, such as those for ionization of H_2 [9], which use distorted waves in all channels are likely to model the recoil scattering more successfully. In Ref. [9], the authors compared their theoretical results for the TDCS for electron-impact ionization of H_2 with experimental data of Jung *et al.* [2]. Unfortunately, no measurements of the recoil region were available, and hence in the comparison, the angular range from 180° to 360° was not plotted. However, there is an indication of the onset of a substantial recoil peak in the theory.

The present results demonstrate that considerable theoretical development is still required in order to accurately model such a fundamental process as electron-impact ionization of the water molecule. The results highlight the fact that although, as in this case, comparison of the theoretical predictions with integrated cross sections like the SDCS exhibited very satisfactory agreement, there can be large discrepancies between theory and experiment for more highly differential cross sections, depending upon the choice of kinematics. This can have major implications in applications where accurate knowledge of the angular distribution of the emitted electrons is an important factor. Future theoretical work on this problem will be directed at incorporating distorted waves into all channels of the process.

[1] M. Coplan, J. H. Moore, and J. P. Doering, Rev. Mod. Phys. **66**, 985 (1994).
[2] K. Jung, E. Schubert, D. A. L. Paul, and H. Ehrhardt, J. Phys. B **8**, 1330 (1975).
[3] M. Chérid, A. Lahmam-Bennani, A. Duguet, R. Zurales, R. Lucchese, M. Dal Cappello, and C. Dal Cappello, J. Phys. B **22**, 3483 (1989).
[4] L. Avaldi, R. Camilloni, E. Fainelli, and G. Stefani, J. Phys. B **25**, 3551 (1992).
[5] J. P. Doering and J. Yang, Phys. Rev. A **54**, 3977 (1996).
[6] S. Rioual, V. Nguyen, and A. Pochat, Phys. Rev. A **54**, 4968 (1996).
[7] S. J. Cavanagh and B. Lohmann, J. Phys. B **32**, L261 (1999).
[8] J. Yang and J. P. Doering, Phys. Rev. A **63**, 032717 (2001).
[9] A. L. Monzani, L. E. Machado, M.-T. Lee, and A. M. Machado, Phys. Rev. A **60**, R21 (1999).
[10] C. Champion, J. Hanssen, and P. A. Hervieux, Phys. Rev. A **65**, 022710 (2002).
[11] R. Cambi, G. Ciullo, A. Sgamellotti, C. E. Brion, J. P. D. Cook, I. E. McCarthy, and E. Weigold, Chem. Phys. **91**, 373 (1984).
[12] A. O. Bawagan, L. Y. Lee, K. T. Leung, and C. E. Brion, Chem. Phys. **99**, 367 (1985).
[13] B. Boudaiffa, P. Cloutier, D. Hunting, M. A. Huels, and L. Sanche, Science **287**, 1658 (2000).
[14] S. J. Cavanagh and B. Lohmann, Phys. Rev. A **57**, 2718 (1998).
[15] P. M. Johnson, S. D. Beames, S. Bell, and B. Lohmann, Rev. Sci. Instrum. **65**, 3178 (1994).
[16] M. A. Haynes and B. Lohmann, J. Phys. B **33**, 4711 (2000).